

## STRUCTURE NOTE

# Crystal structure of tflp: A ferredoxin-like metallo- $\beta$ -lactamase superfamily protein from *Thermoanaerobacter tengcongensis*

Shen-Yan Gu, Xiao-Xue Yan, and Dong-Cai Liang\*

National Laboratory of Biomacromolecules, Institute of Biophysics, Chinese Academy of Sciences, Beijing, People's Republic of China

**Key words:** metallo- $\beta$ -lactamase superfamily; ferredoxin; [Fe-S] cluster; ultraviolet/visible spectroscopy; electronic paramagnetic resonance spectroscopy.

### INTRODUCTION

Ferredoxins are a group of proteins containing non-heme iron and acid-labile sulfur. They are ubiquitous electron transfer proteins participating in a wide variety of redox reactions. Many organisms express multiple ferredoxins.<sup>1</sup> Three types of [Fe-S] clusters have been described so far in ferredoxins: [2Fe-2S], [3Fe-4S], and [4Fe-4S]. The structures of these [Fe-S] clusters have substantial inherent stability in anaerobic solution, but oxygen can convert the exposed [Fe-S] clusters to unstable forms that decompose rapidly. Because of the high affinity of iron for thiolate residue, cysteine residue is the most common ligand of the Fe atom, but some other amino acid residues including histidine, aspartate, serine, and even backbone amide have also been found to coordinate the iron.<sup>2</sup>

Despite the limited [Fe-S] cluster types, ferredoxins present largely diverse structural architectures.<sup>3</sup> A group of metallo- $\beta$ -lactamase superfamily (MBLs) proteins were found to be ferredoxins bearing [2Fe-2S] cluster, but their crystal structures have not been reported.<sup>4</sup> Here we report the crystal structure of a ferredoxin-like protein from *Thermoanaerobacter tengcongensis* (Tflp). Although Tflp is considered as a member of MBLs based on its three-dimensional structural similarity, its crystal structure represents some novel structural features. A novel structural motif comprising four antiparallel  $\beta$  strands is found and a di-Fe center is located in the conserved active site.

Tflp is one of the 15 proteins in *T. tengcongensis* considered to be unique to thermophiles.<sup>5</sup> The gene encoding Tflp clusters with another six genes encoding

ferredoxins. The ultraviolet/visible (UV/Vis) and electronic paramagnetic resonance (EPR) spectra reveal the existence of a [Fe-S] cluster in Tflp reconstituted with sulfur and iron under dithionite-reduced condition. These results characterize Tflp as a kind of ferredoxin.

### MATERIALS AND METHODS

#### Cloning, expression, and purification

The ORF of Tflp (NCBI Accession No. AE013140) from *T. tengcongensis* genome<sup>6</sup> was amplified by PCR and cloned into the pQE30 vector using the restriction sites *Bam*H I and *Hind* III to allow its expression as a fusion protein with a N-terminal 6 $\times$  His-tag. Tflp was over-expressed in *E. coli* strain M15. The bacterial pellet was lysed by sonication in buffer A (30 mM sodium phosphate pH 7.5, 400 mM NaCl) supplemented with 50 mM imidazole. After centrifugation at 4°C, 25,000g for 0.5 h to remove cell debris, the supernatant was loaded onto a Ni-chelated affinity chromatography column (Amersham Biosciences). The protein was eluted with buffer A supplemented with 300 mM imidazole, the

Grant sponsor: National Basic Research Program; Grant numbers: 2002CB713801, 2006CB806501; Grant sponsor: National Protein Project; Grant numbers: 2006CB910902, 2007CB914302.

\*Correspondence to: Dong-Cai Liang, National Laboratory of Biomacromolecules, Institute of Biophysics, Chinese Academy of Sciences, 15 Datun Road, Chaoyang District, Beijing 100101, People's Republic of China.

E-mail: dcliang@sun5.ibp.ac.cn

Received 1 February 2008; Revised 21 February 2008; Accepted 28 February 2008

Published online 22 April 2008 in Wiley InterScience (www.interscience.wiley.com). DOI: 10.1002/prot.22069

**Table I**  
Data Collection, Phasing, and Refinement Statistics for Tflp Structures

	Native	Cd-derivative
<i>Data collection statistics</i>		
Wavelength (Å)	1.5418	1.5418
Resolution (Å)	15–2.1	15–2.8
The highest resolution shells (Å)	2.15–2.10	2.88–2.80
Space group	P2 <sub>1</sub> 2 <sub>1</sub> 2	P2 <sub>1</sub> 2 <sub>1</sub> 2
Unit cell parameters	$a = 77.2, b = 138.3, c = 52.9 \text{ \AA}$ $\alpha = \beta = \gamma = 90^\circ$	$a = 76.7, b = 137.4, c = 53.5 \text{ \AA}$ $\alpha = \beta = \gamma = 90^\circ$
No. unique reflections	30,860	14,530
Redundancy	10	14
Completeness (%)	93 (70)	96 (90)
$R_{\text{merge}}$ (%)	7.8 (35)	10.0 (45)
Percentage of data with $I/\sigma(I) > 3$	76 (40)	75 (43)
<i>Refinement statistics</i>		
Nonhydrogen atoms	4,576	
Protein	4,378	
Water	198	
Fe <sup>3+</sup>	4	
No. unique reflections (test)	1650	
$R_{\text{work}}$ (%)	20.0	
$R_{\text{free}}$ (%)	21.9	
r.m.s.d.		
Bond length (Å)	0.010	
Bond angle (°)	1.293	
Overall average B factor (Å <sup>2</sup> )	25.7	
Main chain B factor (Å <sup>2</sup> )	24.7	
Side chain B factor (Å <sup>2</sup> )	26.3	
Ramachandran plot		
Most favored regions (%)	88.8	
Allowed regions (%)	9.4	
Generously allowed regions (%)	1.2	
Disallowed regions (%)	0.6	

eluent containing Tflp was pooled and dialyzed against buffer B (20 mM sodium phosphate pH 6.5) at 4°C for 12 h. The solution enriched with Tflp was loaded onto a ResourceTM S (1 mL) ion-exchange column (Amersham Biosciences), and then Tflp was eluted in buffer B with NaCl at a linear gradient concentration of 0–1 M. The fractions containing pure Tflp were concentrated to approximately 40 mg/mL and stored at –80°C.

### Crystallization and diffraction data collection

Tflp was crystallized at 20°C by hanging-drop vapor-diffusion method. The hanging drops were made by mixing 2 µL of protein solution with 2 µL of reservoir solution (24.5% pentaerythritol propoxylate (5/4 PO/OH), 100 mM Bis-Tris pH 6.5, and 80 mM ammonium acetate). Reservoir solution containing 30% pentaerythritol propoxylate (5/4 PO/OH) was used as mother liquor and cryoprotectant. Tflp crystals were flash-frozen directly in liquid nitrogen. The diffraction data were collected on a Rikagu R-axis IP IV<sup>++</sup> detector. All data were indexed, integrated, and scaled with the HKL program.<sup>7</sup> The statistics of the data are summarized in Table I.

### Structure determination and refinement

Heavy-atom derivatives were obtained by soaking the crystals in mother liquor supplemented with 2 mM CdCl<sub>2</sub> for 48 h. Tflp structure was determined by SIRAS method using the SHARP program.<sup>8</sup> OASIS2006<sup>9</sup> and ARP/wARP<sup>10</sup> were used to improve the phase and build the model. The structural model was then refined by REFMAC5.<sup>11</sup> The COOT program was used in manual model adjustment.<sup>12</sup> The statistics of the refinement and stereochemistry of the final model are listed in Table I. The coordinates and structure factors of Tflp were deposited into the Protein Data Bank (PDB) with accession code **2P4Z**.

### Reconstitution of the [Fe-S] cluster

The protocol for the reconstitution of [Fe-S] cluster has been described by Heinnickel *et al.*<sup>13</sup> Tflp under dithionite-reduced condition was incubated with 1 mM FeCl<sub>3</sub> in 20 mM phosphate buffer (pH 7.0) for 20 min. Subsequently, Na<sub>2</sub>S was added to a final concentration of 1 mM. And some controls are also carried out in parallel: sample A, Tflp in solution with 1 mM FeCl<sub>3</sub> and 1 mM

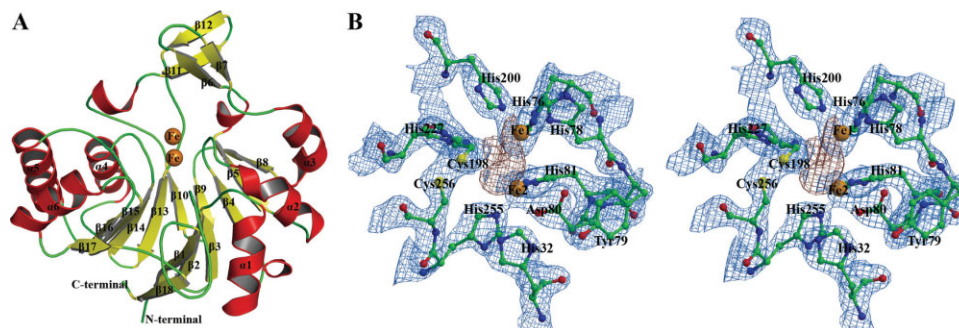


**Figure 1**

Overall structure and active site of Tflp. (A) The  $\alpha$ -helices and  $\beta$  strands are shown in red and yellow, respectively. The Fe atoms are shown in brown. The image was made with PyMol (<http://www.pymol.org>). (B) Stereo view of the active site. The [2Fe-Fe] electron density map contoured at 1.5 sigma (blue) and [Fe-Fe] electron density map contoured at 3.5 sigma (brown) are shown. The image was made with MolScript (<http://www.avatar.se/molscript/>).

Na<sub>2</sub>S and exposed to air for 2 h; sample B, Tflp under dithionite-reduced condition for 2 h; sample C, Tflp with 1 mM FeCl<sub>3</sub> under dithionite-reduced condition for 2 h; sample E, Tflp with 1 mM Na<sub>2</sub>S under dithionite-reduced condition for 2 h; sample D, F, G, Tflp with 1 mM FeCl<sub>3</sub> and 1 mM Na<sub>2</sub>S under dithionite-reduced condition for 0.5, 1, 2 h, respectively. The protein concentration was approximately 30 mg/mL. These samples were centrifuged at 30,000g for 10 min at 25°C before the UV/Vis and EPR experiment.

### UV/Vis spectroscopy

The spectra of Tflp samples in 1-mL quartz cuvettes were recorded by a Hitachi U-3010 spectrophotometer at room temperature. The wavelength scan range is 290–800 nm.

### Low-temperature X-band EPR spectroscopy

Low-temperature EPR spectroscopy was performed using a Bruker ESP-300 Electron Spin Resonance Spectrometer. The EPR experimental conditions were as follows: temperature, 77 K; power, 50 mW; microwave frequency, 9.41 GHz; receiver gain,  $1 \times 10^4$ ; and modulation amplitude, 12 G at 100 kHz. Tflp samples for EPR were concentrated to approximately 180 mg/mL, which was fivefold higher than that of the samples used in UV/Vis spectroscopy.

## RESULTS AND DISCUSSION

### Sequence analysis of Tflp

The gene encoding Tflp is not separated in the *T. tengcongensis* genome. We searched for the annotation of the operon containing the Tflp-encoded gene through SHOPS Server and TIGR Server,<sup>14,15</sup> and learned that

the gene encoding Tflp is located in the putative polycistronic operon together with a series of genes including *tte1887*, *tte1888*, *tte1890*, *tte1891*, *tte1892*, and *tte1893*. The *tte1887* encodes a ferredoxin containing a [4Fe-4S] cluster-binding domain. The *tte1888*, *tte1890*, and *tte1893* encode a family of iron-molybdenum cluster-binding proteins. The *tte1891* and *tte1892* encode the P-loop ATPases containing an inserted ferredoxin domain. The result suggests that Tflp is a kind of ferredoxin.

### Overall structure of Tflp: A novel member in MBLs

Tflp crystals belong to space group P2<sub>1</sub>2<sub>1</sub>2. The structure was refined against diffraction data up to 2.1 Å. Two molecules form a homodimer that contains 551 of the expected 568 amino acid residues in an asymmetric unit. The N-terminal nine residues in molecule A and eight residues in molecule B are absent in the model due to their poor electron density. The two Tflp molecules in the dimer are very similar to each other with a root mean square deviation (r.m.s.d) of 0.18 Å for all corresponding pairs of the C $\alpha$  atoms. They are related by a noncrystallographic twofold axis, and the  $\beta_1$ - $\beta_2$  loop and  $\alpha_6$  helix of each molecule form the interface between the two molecules. Each protein molecule is associated with two Fe ions.

Despite the low amino acid sequence identity with other MBLs members, the Tflp structure contains a 4-layer  $\alpha\beta/\beta\alpha$  sandwich architecture [Fig. 1(A)] that is normal in other MBLs members. The six  $\alpha$ -helices are exposed to the solvent and surround a compact core composed of two layers of  $\beta$  strands. The first four  $\beta$  strands are antiparallel and the subsequent three are parallel in each layer of the  $\beta$  strands.

A striking feature of Tflp is that it contains an independent motif, which is not seen in other MBLs members. This motif is composed of four antiparallel  $\beta$

strands ( $\beta_6$ ,  $\beta_7$ ,  $\beta_{11}$ , and  $\beta_{12}$ ), and they form a lid covering the active site. Structural search using the Dali Server<sup>16</sup> did not reveal any similar motif in the three-dimensional structure database. So this antiparallel four- $\beta$ -strand motif is a novel three-dimensional motif.

Three closest structural homologies of Tflp found by three-dimensional structural alignment using the Dali Server<sup>16</sup> are DNA/RNA processing enzymes. However, the two Fe atoms found in Tflp structure are not seen in these DNA/RNA processing enzymes.

### Characteristics of Tflp active site

Most MBLs members contain a conserved metal binding site in the cavity at the interface between the two layers of  $\beta$  strands. This metal binding site always acts as the active site in MBLs. The residues coordinating the metal ions in this active site form a conserved sequence motif H-x-[EH]-x-D-[CRSH]-x<sub>n</sub>-H-x<sub>n</sub>-[CSD]-x<sub>n</sub>-H.<sup>17</sup> The electron density map of Tflp also indicates the presence of two metals in the active site [Fig. 1(B)]. Inductively Coupled Plasma Atomic Emission Spectrometry (ICP) of Tflp solution revealed the predominant presence of Fe ions with little Ni and Zn ions. The Ni ions were probably introduced in the Ni-chelated affinity chromatography during the purification, while neither Fe nor Zn ions were added during purification and crystallization. We speculate that Fe and Zn were introduced from the LB medium during protein expression. In the di-Fe center of Tflp, the distance between Fe<sub>1</sub> and Fe<sub>2</sub> is 3.7 Å. The conserved residues His76 (NE2), His78 (ND1), and His200 (NE2) coordinate Fe<sub>1</sub> with distances of 2.3, 2.2, and 2.0 Å, respectively, and Asp80 (OD2), His81 (NE2), and His255 (NE2) coordinate Fe<sub>2</sub> with distances of 2.0, 2.2, and 2.4 Å, respectively. Fe coordinated only by three histidine residues in the di-metal site is rarely seen in MBLs. Besides histidine residues, at least one aspartate or glutamate residue is usually involved in coordination to Fe in MBLs.<sup>18</sup> However, in the di-metal site of Tflp, only three histidine residues coordinate to Fe<sub>1</sub>. We performed a three-dimensional pattern search with the key residues in the di-metal site using the Pints Server.<sup>19</sup> The closest structural homolog to the di-metal site of Tflp is flavo-protein A from *Moorella thermoacetica* (PDB code 1ycf), which also contains a di-Fe center.

The disulfide bond approximating to the di-Fe center in the active site is unique among the MBLs members with known structures. Two cysteine residues (Cys198 and Cys256) form a disulfide bond with a bond length of 2.1 Å. The [2Fo-Fc] and [Fo-Fc] electron density maps show that Cys198, an important residue in the active site, exists in alternative conformations. Cys198 forms the disulfide bond with Cys256 in its major conformation, while it interacts with Fe<sub>1</sub> with a distance of 2.3 Å in the minor conformation [Fig. 1(B)]. The formation of the disulfide bond under air-oxidized condition probably

results in a movement of His255 toward Fe<sub>2</sub>, thereby further lower the affinity of the protein for Fe<sub>2</sub>.

### Spectral characteristics of Tflp

Tflp reconstituted with iron and sulfur under dithionite-reduced condition changed its color to greenish brown within 3 h and then bleached upon prolonged exposure to air for several hours. The color change is similar to that of pyruvate formate-lyase-activating enzyme from *E. coli* reconstituted with [Fe-S].<sup>20</sup> UV/Vis spectroscopy was performed on Tflp sample A - G. The UV/Vis absorption spectra of Tflp samples (D, E, F, and G) were found to have pronounced shoulders at 420, 523, and 615 nm [Fig. 2(A)]. The absorption maximum at 420 nm is a typical feature of [Fe-S] clusters, and the peaks at 523 and 615 nm result from the transient formation of Fe<sub>x</sub>S<sub>y</sub> compounds,<sup>21,22</sup> which indicate the formation of some [Fe-S] cluster. The spectra of Tflp reconstituted with [Fe-S] are also similar to those of bovine adrenal ferredoxin containing a [2Fe-2S] cluster when it is in a buffer containing sulfide and mercaptoethanol.<sup>23</sup> The spectrum of sample E (without FeCl<sub>3</sub>) shares the similar feature of sample D, F, and G because of the inherent existence of Fe ions in Tflp. The height of the absorption peak of Tflp at 420 nm gradually increased during prolonged exposure to air [Fig. 2(A), trace d, f, g], which shows the conversion of the [Fe-S] cluster from the reduced state to the oxidized state.<sup>20</sup> These spectral data indicate that the inorganic sulfur and dithionite are indispensable for the appearance of the absorption maxima.

Low-temperature EPR analysis was performed on the reconstituted [Fe-S] cluster of Tflp. The apparent  $g_x$ ,  $g_y$ , and  $g_z$  values of the overall EPR signal are approximately 2.04, 1.99, and 1.91, respectively [Fig. 2(B)]. These  $g$  values are in high accordance with those of the ferredoxin from *Haloferax mediterranei* ( $g_x = 2.07$ ,  $g_y = 1.98$ , and  $g_z = 1.91$ ),<sup>24</sup> and are very similar to those of the heterodisulfide reductase (Hdr)-like protein from the sulfate-reducing archaeon *A. fulgidus* ( $g_x = 2.03$ ,  $g_y = 1.99$ , and  $g_z = 1.95$ ).<sup>25</sup> The same  $g_y$  value of 1.99 has also been observed in Hdr from methanogenic archaea which contains a [Fe-S] cluster.<sup>26</sup> The EPR spectra provide powerful evidence for the existence of a [Fe-S] cluster, but the specific type of the [Fe-S] cluster cannot be determined in this experiment.

To summarize, we found a di-Fe center and a neighboring disulfide bond in the crystal structure of Tflp. Meanwhile, the UV/Vis and EPR spectra definitely indicate the existence of a reconstituted [Fe-S] cluster in Tflp. Taken together, we conclude that a [Fe-S] cluster was reconstituted with inorganic sulfur and iron in the active site under dithionite-reduced condition. And the di-Fe center in the crystal structure is the remaining part of that [Fe-S] cluster, because oxygen can destabilize the

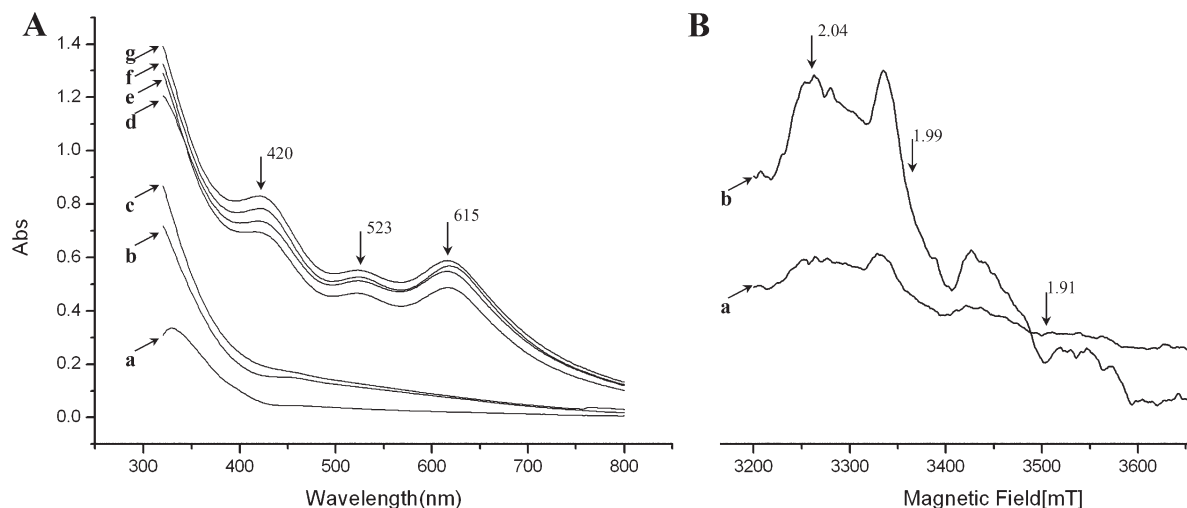


**Figure 2**

UV/Vis and EPR spectra of reconstituted Tflp. (A) UV/Vis spectra of Tflp under different conditions. The arrows indicate the absorption maxima. Trace a–g corresponds to the sample A–G, respectively. (B) Low-temperature EPR spectra of the sample G with higher protein concentration. Trace a, the EPR signal of one measurement; trace b, the signal averaging by digitally accumulating four measurements.

[Fe-S] cluster *in vitro*. Moreover, the sequence analysis shows that the gene encoding Tflp is located in an operon containing a series of genes encoding ferredoxins. All these indicate that Tflp is a kind of ferredoxin. Although the specific type of the [Fe-S] cluster in Tflp has not been determined, we speculate it to be a novel type due to the unique protein ligands. These ligands including five histidine residues (His76, His78, His200, His81, and His255) and one aspartate residue (Asp80) are not described before.

## ACKNOWLEDGMENTS

thank Professor Jing-Fen Lu of Peking University for her expert technical assistance in EPR Spectroscopy. They thank Professor Run-Sheng Chen of the Institute of Biophysics of CAS for kindly providing the *T. tengcongensis* strain.

## REFERENCES

- Clements AP, Ferry JG. Cloning, nucleotide sequence, and transcriptional analyses of the gene encoding a ferredoxin from *Methanosarcina thermophila*. *J Bacteriol* 1992;174:5244–5250.
- Imlay JA. Iron-sulphur clusters and the problem with oxygen. *Mol Microbiol* 2006;59:1073–1082.
- Sticht H, Rosch P. The structure of iron-sulfur proteins. *Prog Biochem Mol Biol* 1998;70:95–136.
- Daiyasu H, Osaka K, Ishino Y, Toh H. Expansion of the zinc metallo-hydrolase family of the beta-lactamase fold. *FEBS Lett* 2001;503:1–6.
- Bao Q, Tian Y, Li W, Xu Z, Xuan Z, Hu S, Dong W, Yang J, Chen Y, Xue Y, Xu Y, Lai X, Huang L, Dong X, Ma Y, Ling L, Tan H, Chen R, Wang J, Yu J, Yang H. A complete sequence of the *T. tengcongensis* genome. *Genome Res* 2002;12:689–700.
- Zeng G. Sticky-end PCR: new method for subcloning. *Biotechniques* 1998;25:206–208.
- Otwinowski Z, Minor W. Processing of X-ray diffraction data collected in oscillation mode. In: *Methods in enzymology*, Vol. 276: Macromolecular crystallography, part A; 1997. pp 307–326.
- Vonrhein C, Blanc E, Roversi P, Bricogne G. Automated structure solution with autoSHARP. *Methods Mol Biol* 2006;364:215–230.
- Yao DQ, Huang S, Wang JW, Gu YX, Zheng CD, Fan HF, Watanabe N, Tanaka I. SAD phasing by OASIS-2004: case studies of dual-space fragment extension. *Acta Crystallogr D Biol Crystallogr* 2006; 62:883–890.
- Perrakis A, Morris R, Lamzin VS. Automated protein model building combined with iterative structure refinement. *Nat Struct Biol* 1999;6:458–463.
- Murshudov GN, Vagin AA, Dodson EJ. Refinement of macromolecular structures by the maximum-likelihood method. *Acta Crystallogr D Biol Crystallogr* 1997;53:240–255.
- Emsley P, Cowtan K. Coot: model-building tools for molecular graphics. *Acta Crystallogr D Biol Crystallogr* 2004;60:2126–2132.
- Heinrich M, Shen G, Agalarov R, Golbeck JH. Resolution and reconstitution of a bound Fe-S protein from the photosynthetic reaction center of *Heliobacterium modesticaldum*. *Biochemistry* 2005;44:9950–9960.
- van Bakel H, Huynen M, Wijmenga C. Prokaryotic diversity of the *Saccharomyces cerevisiae* Atx1p-mediated copper pathway. *Bioinformatics* 2004;20:2644–2655.
- Ermolaeva MD, White O, Salzberg SL. Prediction of operons in microbial genomes. *Nucleic Acids Res* 2001;29:1216–1221.
- Holm L, Sander C. Dali: a network tool for protein structure comparison. *Trends Biochem Sci* 1995;20:478–480.
- Gomes CM, Frazao C, Xavier AV, Legall J, Teixeira M. Functional control of the binuclear metal site in the metallo-beta-lactamase-like fold by subtle amino acid replacements. *Protein Sci* 2002; 11:707–712.
- Schilling O, Wenzel N, Naylor M, Vogel A, Crowder M, Makaroff C, Meyer-Klaucke W. Flexible metal binding of the metallo-beta-



- lactamase domain: glyoxalase II incorporates iron, manganese, and zinc in vivo. *Biochemistry* 2003;42:11777–11786.
19. Stark A, Sunyaev S, Russell RB. A model for statistical significance of local similarities in structure. *J Mol Biol* 2003;326:1307–1316.
  20. Kulzer R, Pils T, Kappl R, Huttermann J, Knappe J. Reconstitution and characterization of the polynuclear iron-sulfur cluster in pyruvate formate-lyase-activating enzyme. Molecular properties of the holoenzyme form. *J Biol Chem* 1998;273:4897–4903.
  21. Leal SS, Teixeira M, Gomes CM. Studies on the degradation pathway of iron-sulfur centers during unfolding of a hyperstable ferredoxin: cluster dissociation, iron release and protein stability. *J Biol Inorg Chem* 2004;9:987–996.
  22. Pieck JC, Hennecke U, Pierik AJ, Friedel MG, Carell T. Characterization of a new thermophilic spore photoproduct lyase from *Geobacillus stearothermophilus* (SplG) with defined lesion containing DNA substrates. *J Biol Chem* 2006;281:36317–36326.
  23. Burova TV, Beckert V, Uhlmann H, Ristau O, Bernhardt R, Pfeil W. Conformational stability of adrenodoxin mutant proteins. *Protein Sci* 1996;5:1890–1897.
  24. Martinez-Espinosa RM, Richardson DJ, Butt JN, Bonete MJ. Spectropotentiometric properties and salt-dependent thermotolerance of a [2Fe-2S] ferredoxin-involved nitrate assimilation in *Haloflex mediterranei*. *FEMS Microbiol Lett* 2007;277:50–55.
  25. Mander GJ, Duin EC, Linder D, Stetter KO, Hedderich R. Purification and characterization of a membrane-bound enzyme complex from the sulfate-reducing archaeon *Archaeoglobus fulgidus* related to heterodisulfide reductase from methanogenic archaea. *Eur J Biochem* 2002;269:1895–1904.
  26. Madadi-Kahkesh S, Duin EC, Heim S, Albracht SP, Johnson MK, Hedderich R. A paramagnetic species with unique EPR characteristics in the active site of heterodisulfide reductase from methanogenic archaea. *Eur J Biochem* 2001;268:2566–2577.